Proceedings of ASME TURBO EXPO 2012
Power for Land, Sea and Air
June 11 – 15, 2012, Copenhagen, Denmark

GT2012-68588

MAIN ANNULUS GAS PATH INTERACTIONS - TURBINE STATOR WELL HEAT TRANSFER

Jeffrey A. Dixon, Antonio Guijarro Valencia
Rolls-Royce plc, Derby, UK

Daniel Coren, Visiting Research Fellow
Department of Mechanical Engineering Imperial College London

Daniel Eastwood, Christopher Long
TFMRC, University of Sussex, Brighton, UK

ABSTRACT

This paper summarises the work of a 5-year research programme into the heat transfer within cavities adjacent to the main annulus of a gas turbine. The work has been a collaboration between several gas turbine manufacturers, also involving a number of universities working together. The principal objective of the study has been to develop and validate computer modelling methods of the cooling flow distribution and heat transfer management, in the environs of multi-stage turbine disc rims and blade fixings, with a view to maintaining component and sub-system integrity, whilst achieving optimum engine performance and minimising emissions.

A fully coupled analysis capability has been developed using combinations of commercially available and in-house computational fluid dynamics (CFD) and finite element (FE) thermo-mechanical modelling codes. The main objective of the methodology is to help decide on optimum cooling configurations for disc temperature, stress and life considerations. The new capability also gives us an effective means of validating the method by direct use of disc temperature measurements, where otherwise, additional and difficult to obtain parameters, such as reliable heat flux measurements, would be considered necessary for validation of the use of CFD for convective heat transfer.

A two-stage turbine test rig has been developed and improved to provide good quality thermal boundary condition data with which to validate the analysis methods. A cooling flow optimisation study has also been performed to support a re-design of the turbine stator well cavity, to maximise the effectiveness of cooling air supplied to the disc rim region. The benefits of this design change have also been demonstrated on the rig. A brief description of the test rig facility will be provided together with some insights into the successful completion of the test programme. Comparisons will be provided of disc rim cooling performance, for a range of cooling flows and geometry configurations.

The new elements of this work are the presentation of additional test data and validation of the automatically coupled analysis method applied to a partially cooled stator well cavity, (i.e. including some local gas ingestion); also the extension of the cavity cooling design optimisation study to other new geometries.

INTRODUCTION

The requirement for ever more efficient gas turbine engines is leading to increased gas path temperatures, creating increasingly hostile environmental conditions for the adjacent turbomachinery and support structures. Cooling air systems are designed to protect vulnerable components from the hot gas that would otherwise be entrained into the cavities communicating with the main annulus, through the inevitable gaps between rotating and static parts. These cooling flows are bled from the compressor stages and reduce the engine efficiency as they can represent around 20% of the total main gas path flow. These performance penalties manifest themselves in two ways, i.e. having a direct impact on thermodynamic cycle performance, resulting from imperfect work extraction in the turbines, and in the spoiling effect of the efflux at the point where it re-enters the turbine main annulus flow, causing a reduction in stage efficiency. It is desirable therefore to minimise these cooling flows, to levels consistent with maintaining the optimum component lives and the mechanical integrity of the engine. The various cooling air and gas flows involved are illustrated for a typical multi-stage turbine, in Figure 1.

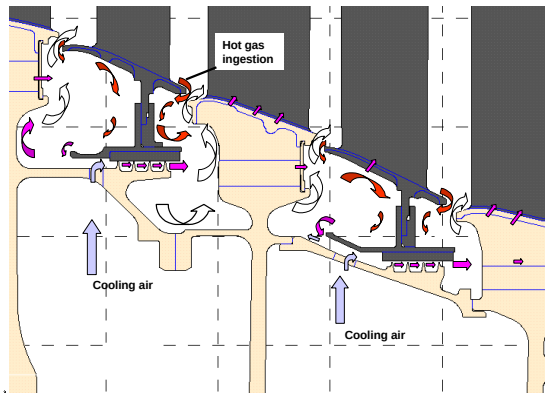

Figure 1 Typical turbine stator well

Under the auspices of the European Commission Programme for Research and Technological Development Framework 6 - Aeronautics and Space, a consortium of European gas turbine manufacturers and universities has undertaken a five-year project to address this specific issue. This project was called Main Annulus Gas Path Interactions or MAGPI [1], now complete. There were 5 work-packages in this project and the first of these was specifically aimed at turbine disc rim cavity heat transfer and cooling optimisation. This work was built on a previous study [2], both extending the methodology, and improving the quality of the test data used to validate the method.

This paper presents a description of the rig test facility and the numerical analysis work performed by one of the partners in the consortium, with references to the work of other partners, and summarises the conclusions and lessons learned from the research programme. The aim of the work was to further advance the understanding of cooling flow, annulus gas interaction and resultant heat transfer, in the cavities adjacent to the main annulus in multi-stage turbines; in particular:-

- The flow distribution and mixing which take place in the turbine stator well.
- The influence of the geometrical features such as cooling air entry holes and interstage seal clearance.
- The opportunities for improving the effectiveness of the cooling air, such as the entry location and the introduction of a deflector plate.
- The interaction between the disc rim boundary layer and the main annulus gas ingestion flows.

Finite element and computational fluid dynamics models have been created and up-dated to improve the analysis tool-set and best practices for turbine stator well design. A coupled analysis technique [3] has been further developed, which enables the direct application of convective heat fluxes generated in the cavity CFD solutions, to be applied to the FE models representing the engine hardware. Reference is also made to the conjugate CFD/FE analysis of another partner in the consortium [4], which greatly helped in the understanding of early observations of the test rig behaviour. These modelling capabilities have been validated using measured data from the two-stage turbine facility sited at the University of Sussex. Both steady and unsteady CFD solutions have been produced during the project, some presented at previous ASME conferences [5] and [6], with comparisons to measured data. Alternative cooling configurations have been both modelled and tested for a range of cooling flow levels. Additional work has been done to improve the effectiveness of the cooling air supplied and to validate the benefits of the design changes introduced.

NOMENCLATURE

h	Surface heat transfer coefficient [W/m^2.K]
R	Gas constant [J/kg.K]
T	Temperature [K]
T_t	Total temperature [K]
θ	Non-dimensional temperature [-]
H	Enthalpy [J/s]
η_{eff}	Thermal cooling effectiveness [-]
η	Isentropic turbine efficiency [-]
p	Fluid static pressure [Pa]
p_t	Fluid total pressure [Pa]
ν	Fluid kinematic viscosity, μ/ρ [m^2/s]
ρ	Fluid density [kg/m^3]
$\dot{m}$	Mass Flow [kg/s]
Ω	Angular velocity [rad/s]
y^+	Non-dimensional wall distance, $\rho.u_\tau.y_P/\mu$ [-]
$_i$	Subscript CFD model inlet
$_o$	Subscript CFD model outlet

THE TEST FACILITY

All tests were carried out at the University of Sussex, Thermo-Fluid Mechanics Research Centre. The test facility is shown in Figure 2. A brief overview is given here; full details can be found in Coren [7] and Eastwood et al [8].

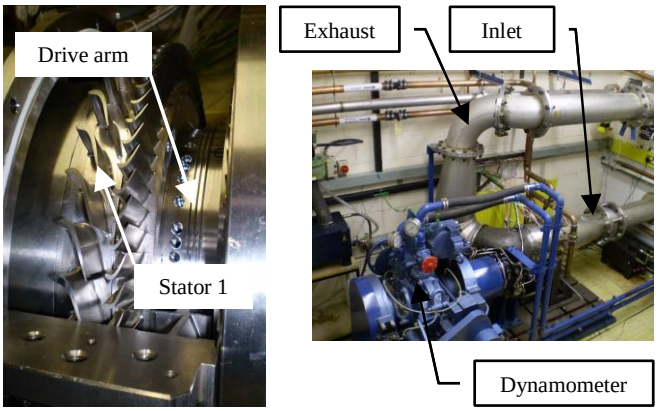

Figure 2 Turbine Rig Test Facility

The test section of the rig comprises a two-stage turbine, rated at 400kW, with a pressure ratio of approximately 2.5 at the design condition. Flow coefficients are 0.51 for stage 1 and 0.62 for stage 2, with work coefficients of 1.6 and 1.4 respectively, which were designed to be representative of a typical multistage low/intermediate pressure turbine. Main annulus air is supplied by an adapted aero engine driven compressor plant at 4.9 kgs^{-1}, 3.3 bar absolute and approximately 170 °C. An Atlas Copco screw type compressor is used to provide the various cooling air supplies.

The cross section of the rig test section (Figure 3) has been designed to represent the key features of a turbine stator well. The turbine has also been designed to suit the subsequent FE and CFD analyses, with 39 nozzle guide vanes and 78 rotor blades for each stage. Thus the analysis models can be set-up at 1/39th of the complete rotor/stator system. In cavity design point rotational Reynolds number is approximately 1.8x10^6.

Cooling Geometry and Supply

The cooling air is supplied to the hub region of the test rig via insulated transfer tubes. The rig has a split casing and is designed to allow rapid geometry changes. The coolant may be introduced to the upstream stator well either radially through removable threaded inserts, or axially through removable cover plates, with slot exits representing lock plate and blade fixing leakage paths. This arrangement allows 0, 13, 26 or 39 flow exits to be used at each entry point, which enables a range of cooling 'jet' velocities for a given coolant flow rate. However only the 0 and 39 hole flow cases have been analysed to-date, due to available time and model size (sector) restrictions. These features are highlighted in Figure 3. In order to achieve accurate metering of coolant to the stator wells, the delivery path is

separated from the outer wheel space by a balance cavity sealed by two labyrinth seals. During testing this cavity is pressure balanced against the higher pressure coolant supply to prevent leakage; effectively forming a blown seal; see Figure 4.

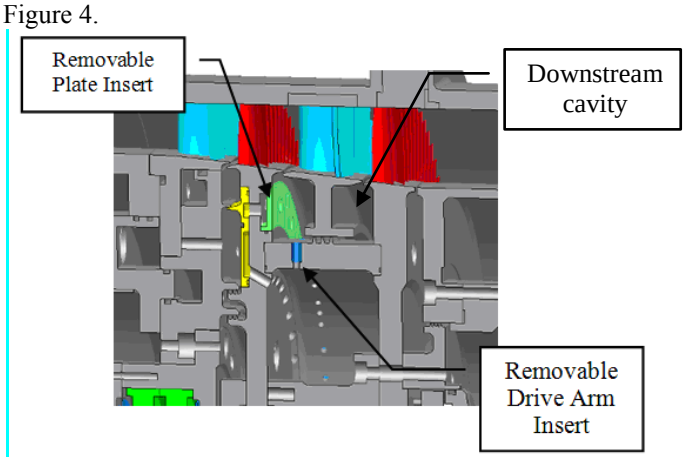

Figure 3 Turbine rig section

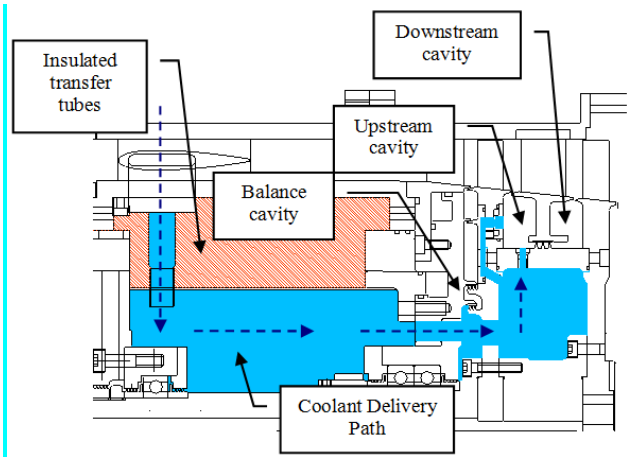

Figure 4 Cooling Flow Paths

The balance air is measured upstream of the rig, and vented from the intermediate wheel-space to prevent egress into the main annulus. This arrangement also allows a known rate of egress to be specified. Cooling air flow rates are determined using hot film air mass meters. Experience in running the rig indicated problems with achieving the required pressure balance across these labyrinth seals, at some of the cooling flow rates in the test matrix. However, having identified the 'problem' flow conditions from the rig instrumentation, it was possible to manage and quantify small leakages without significantly compromising the objectives of the test programme.

Instrumentation

Turbine main annulus conditions are measured by temperature and pressure probes built into the leading edges of the NGVs, avoiding the blade passage restrictions and disturbances inherent with inter-stage probes. The turbine stator well and surrounding regions have been instrumented with metal and air thermocouples and static pressure tappings. The signals from the thermocouples installed on the rotating assembly are transmitted using a 92 channel radio telemetry unit, with custom cold junction referencing, located upstream of the test section. Figures 5 and 6 provide an overview of the test section temperature and pressure instrumentation. More information on the instrumentation is available from Coren [7] and Eastwood [8].

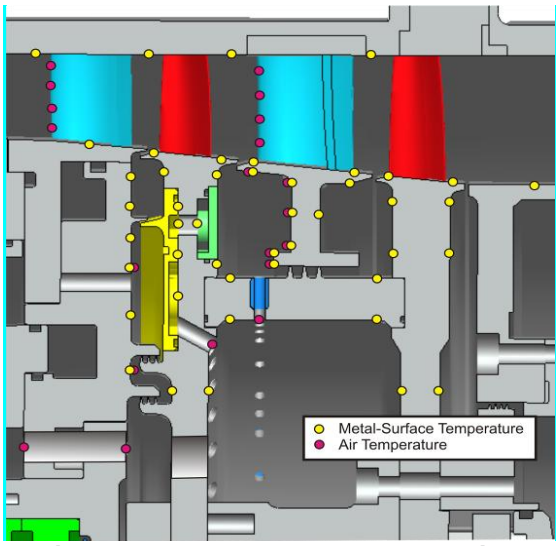

Figure 5 Temperature Instrumentation

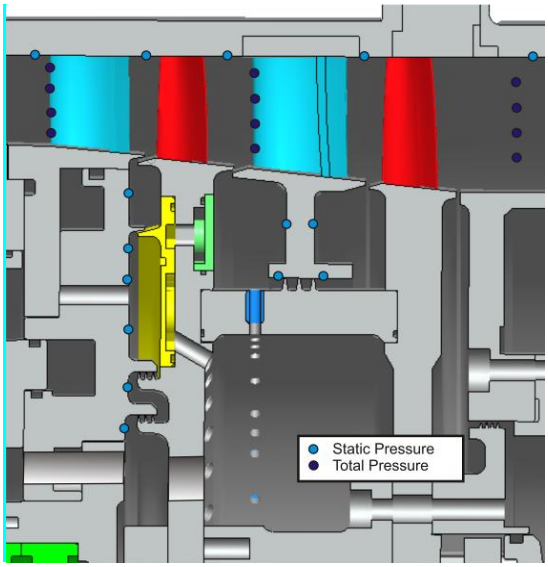

Figure 6 Pressure Measurement Positions

During the course of the analysis of the first phase of the rig test programme it became apparent that it was not possible to reconcile some of the observations from the rig measurements with the predictions of the CFD models. In particular the conjugate CFD model produced by Smith [4], see Figure 7, highlighted a problem with the pressure balancing on the front face of the rotor. On investigation by the team at the rig test facility, it was discovered that some of the 0.8 mm diameter static pressure tapping pipes were leaking through tiny holes caused by a manufacturer's material defect, see Figure 8.

Figure 7 Siemens Conjugate CFD model

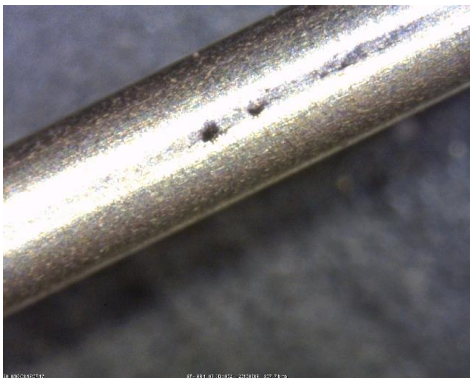

Figure 8 Pressure tapping lead-out pipe flaw

This discovery allowed the rig team to correct early results and complete the remainder of the testing with refurbished instrumentation where required, including repeat testing of the earlier configurations.

NUMERICAL MODELING

The overall objective of this study has been to improve the modelling capability for turbine stator wells, i.e. cooling flow distribution and heat transfer management, with a view to optimising disc rim cooling and component life. As anticipated this has led to further development of the coupled FE/CFD modelling techniques reported in [9, 10 and 11], leading to the development of a validated heat transfer methodology, which has the potential to significantly reduce the requirement for model validation measurements, i.e. engine testing. Based on the now increased confidence in the analysis tool-set, adiabatic CFD solutions have also been used to investigate possible improvements to the design of turbine stator wells, including cooling air placement and geometry changes.

Finite Element Thermo-mechanical Models

In preparation for this objective, FE models of the rig (2D axisymmetric) and test section (3D) were developed. Appropriate solid properties, e.g. thermal conductivity as a function of the metal temperature, are modelled. The 2D model being first used in the rig design phase, Dixon et al [5], to help establish operating temperatures, stress levels and clearances etc. and a full 3D sector model being created to support the validation of the coupled CFD/FE analysis. See Figure 9. This model has been used to reproduce the measured temperatures indicated at the thermocouple positions from the test facility. The CFD solution has been used to replace the more usual, empirical correlation based thermal boundary conditions on the FE model, i.e. to establish the disc rim cavity convective heat transfer (heat fluxes). Together they form the coupled CFD/FE solution, which has then been validated against measured surface temperatures from the test rig.

An in-house computer code SC03 [12] has been used to generate the finite element thermo-mechanical models. The coupling of this code to the commercial CFD analysis program Fluent [13] was reported in [2]. This methodology, first developed by Verdicchio [11], subsequently enhanced in collaboration with the Universities of Sussex and Surrey [9 and 10], is now the chief means of validating the CFD method for convective heat transfer in the stator well. A further development has allowed us to also use an in-house CFD code Hydra [14], for the determination of cooling flow distribution and convective heat transfer, in place of the commercial code.

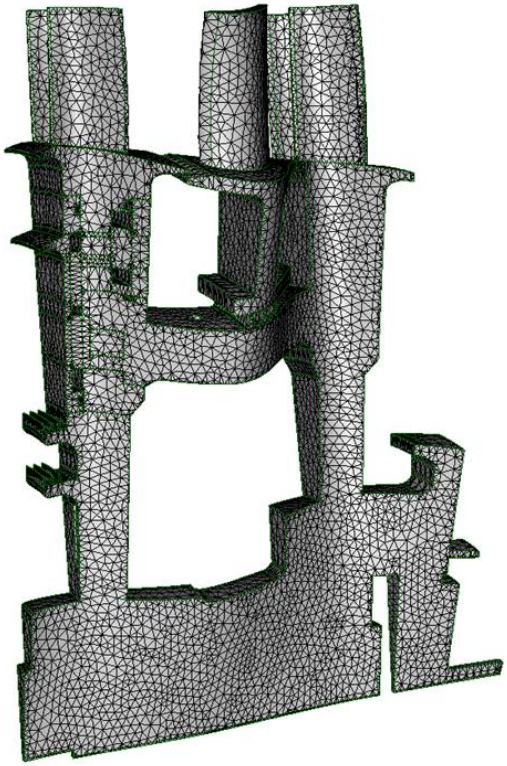

Figure 9 3D Finite Element model (mesh)

Computational Fluid Dynamics Models

In parallel with the development of the test facility, it has been necessary to further extend the CFD modelling capability required to analyze the flow and heat transfer in the turbine stator well. It has now been shown that this may require both steady and unsteady calculations in full 3D, for certain flow conditions, notably where cooling efflux and annulus gas ingestion are finely balanced. However in other flow conditions, e.g. un-cooled stator wells, a steady solution is adequate. The suitability of a sector model chosen to keep the computational requirements within the capability of available computer facilities has now been shown to be adequate, for those areas of the cavity important to control for disc lifing purposes. The test facility was developed with this limitation in mind and the current CFD model is 1/39 of the full rotor/stator system, i.e. incorporating 1 NGV, two rotor blades and one cooling air hole or one ‘lock-plate’ slot.

The CFD mesh was created using the in-house automatic mesh generation software PADRAM. Individual meshes were created for each reference frame region – namely Stator 1, Rotor 1, Stator 2 and Rotor 2 – and loaded and checked in a pre-processor. The primary connectivity mesh is given as an output file. Meshes Rotor 1 and Rotor 2 are merged through the labyrinth seal, to create a rotor fluid single zone, see Figure 10, where the extent of the model has been depicted.

Where possible, a block structured mesh was used, i.e. for all the cases except the deflector plate, where an unstructured mesh was used. This kind of mesh employs a Delaunay triangulation core and an o-grid, which is then swept around the cavity, before connecting to the blade passages. Mesh sensitivity studies have been carried out throughout the duration of the project, until the same solution was achieved with successive grid resolutions. The resulting mesh consisted of about 9 million elements, in

three zones, merged by either mixing planes (steady state solutions), or sliding planes (transient case). As a guideline, around a million cells per blade passage were used, and depending on the case, with between 2.5 and 4 million computational cells for the stator well, always keeping the y+ near unity.

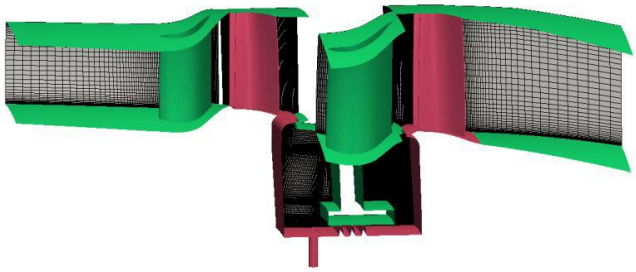

Figure 10 Extent of the computational mesh

Figure 11 shows a detail of the rotor 1 blade leading edge, also depicting the level of near wall spacing achieved. A key area of interest was the rim gap, in order to correctly model the ingestion in that domain. Figure 12 shows a mesh detail of the rotor1-stator2 rim gap, illustrating the level of mesh resolution achieved. Further information on the CFD modelling strategy is provided by Guijarro Valencia in [6].

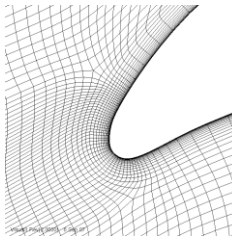

Figure 11

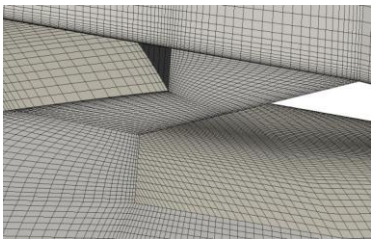

Figure 12

The cavity grid for each geometry is shown in the following pictures: Figure 13 straight drive arm hole; Figure 14 lock plate slot; Figure 15 angled drive arm hole: Figure 16 static deflector plate. The cavity meshing capability has been developed over the course of this five year research programme, e.g. from structured to unstructured meshes, with the usual checks on mesh sensitivity [5] [6].

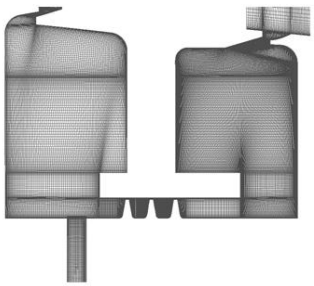

Figure 13

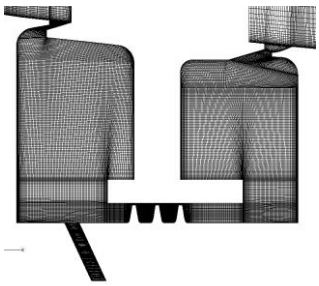

Figure 15

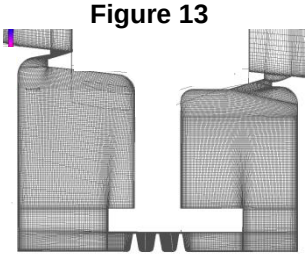

Figure 14

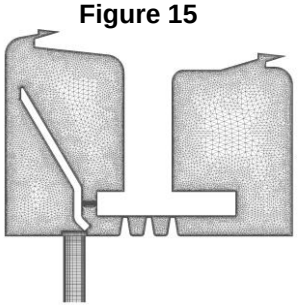

Figure 16

At this stage the in-house CFD analysis code Hydra [14] is used. Note: Other partners in the consortium have used different commercial CFD codes [4 and 15]. Flow and pressure input boundary conditions were as measured on the test facility. The Spalart-Almaras turbulence model [16], with standard wall functions, has been chosen for these calculations. Rolls-Royce plc has extensive successful experience of using Spalart-Almaras for main gas path flows, as well as for fluid flow and heat transfer in secondary flow cavities, using the in-house code. This has allowed benchmarking of the turbulence models used by the MAGPI partners.

The CFD boundary conditions have been generally depicted in Figure 17. For each case, the appropriate test results were used in order to validate the CFD in equivalent conditions. Walls are defined as viscous and hydraulically smooth. The appropriate wall speed for each component is defined. For this analysis, the walls were set to be either adiabatic or, where appropriate, temperature profiles were applied. The main annulus inlet was specified as a mass flow inlet. The cooling air is normally supplied to the test section through a series of holes in the drive arm between Rotor 1 and Rotor 2. These inlet holes are modelled as a mass flow inlet boundary condition, with an applied flow rate. The inlet total temperature was accordingly set to the test measurement taken from the rig experiment. HYDRA uses a V-cycle multi-grid routine, in order to speed up the convergence of the calculation.

OBJECTIVES

The objectives of the modelling capability are to enable the optimum level and placement of cooling air for disc rim environmental control (cooling). This includes the determination of cooling flow re-ingestion, i.e. from the up-stream efflux at the front of the stage 1 disc rim, some of which is drawn into the downstream turbine stator well cavity; see Guijarro [17]. In this paper the most efficient use of the cooling air, i.e. by judicious placement and geometry optimisation, is investigated using adiabatic solutions. The validation of the methodology is also established through the demonstration of the coupled CFD/FE method, by comparisons to the data which have been measured on the test rig at the University of Sussex [8].

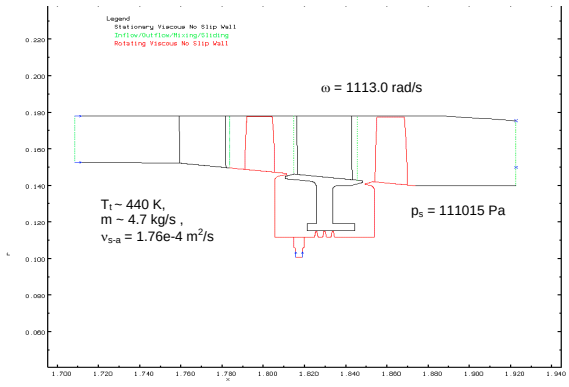

Figure 17 Extent of the CFD geometry showing the operating conditions of the model

The disc surface thermocouple measurements have allowed validation of the method for this application, now that the fully coupled CFD/FE analysis capability has been established, (at least for some flow conditions).

CFD/FE COUPLING

The primary aim of the rig test programme was to generate a good range of high quality test data, which can be used to

assess the capability of the coupled CFD/FE method, to accurately model turbine stator well fluid flow and heat transfer. From the first phase of the test programme an extensive range of accurate and repeatable measurements have been made available for the datum rig geometries, i.e. 'drive arm' cooling holes and 'lock-plate slots'.

In order to be sure of the inlet and exit boundary conditions to the stator well (at the rim gaps), comparisons were made initially with main annulus pressure, temperature and mass-flow measurements. Figure 18 shows the pressure tap and thermocouple rake locations used to compare measured and predicted pressures and temperatures in the main gas path. Test data was first produced for a number of coolant mass flow rates, fed into the stator wall cavity by means of the radial drive arm hole. The mass flow rates are detailed in Table 1. Two representative cases are presented here, i.e. coolant flows of 30 and 55 g/s. The CFD analysis has chiefly been conducted at the rig design point, with measured inlet temperature boundary conditions, to allow better benchmarking with the test data. Table 1 provides more detailed information on the differences between the total pressures and absolute temperatures predicted, with the available measured data. Good agreement has been achieved between the experiments and the CFD simulations. The higher discrepancies were found at the thermocouples in the secondary flows, (i.e. passage vortex predominant). One of the most important sources of error in the early analyses was the difference between the inlet boundary condition initially assumed and the actual inlet temperature. The initial inlet temperature data had been read from a measurement in the DART compressor Venturi tube. However, the measured temperature at the NGV 1 rake is around 1% lower, probably due to heat losses in the inlet system. With this correction, agreement with test data in the main annulus is good. The pressure predictions are also close to the measurements, the maximum difference is less than 3% in the worst case. Thus the main annulus flow solution can be considered to provide suitable boundary conditions at inlet and outlet to the stator well cavity.

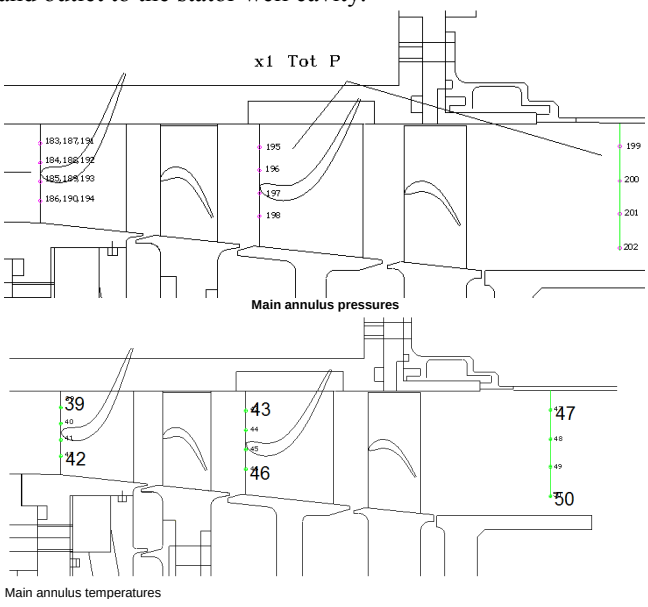

Figure 18 main annulus instrumentation locations

STATOR WELL CAVITY

Air temperature measurements are available from a number of thermocouples located inside the cavity and installed on the stator foot. In the early, 'manual' coupling approach, the metal surface thermocouple data was used to create temperature profiles around the CFD analysis cavity walls.

	Drive Arm Hole, 30 g/s			Drive Arm Hole, 55 g/s		
MA Total Pressure	**Measured**	**CFD**	**delta**	**Measured**	**CFD**	**delta**
Tapping position	(Bar)			(Bar)		
183, 187, 191	2.8790	2.9130	0.034	2.8380	2.8840	0.046
184, 188, 192	2.8920	2.9140	0.022	2.8510	2.8880	0.037
185, 189, 193	2.8890	2.9130	0.024	2.8460	2.8880	0.042
186, 190, 194	2.8890	2.9100	0.021	2.8480	2.8850	0.037
195	1.8511	1.8550	0.004	1.8294	1.8490	0.020
196	1.8374	1.8350	-0.002	1.8147	1.8280	0.013
197	1.8309	1.8300	-0.001	1.8076	1.8240	0.016
198	1.7965	1.8000	0.003	1.7840	1.8090	0.025
MA Total Temperature	**Measured**	**CFD**	**delta**	**Measured**	**CFD**	**delta**
Thermocouple location	(K)			(K)		
39	438.2	440.9	2.7	432.6	437.0	4.4
40	438.9	442.5	3.6	433.3	436.6	3.3
41	439.5	440.7	1.2	433.8	436.0	2.2
43	389.8	396.0	6.2	385.1	391.5	6.4
44	387.8	390.2	2.4	383.0	385.4	2.4
45	387.9	390.4	2.5	383.0	385.0	2.0
46	389.3	393.3	4.0	384.1	388.6	4.5
47	353.0	355.2	2.2	348.0	352.8	4.8
48	352.1	350.7	-1.4	347.1	346.5	-0.6
49	351.9	348.0	-3.9	346.8	344.0	-2.8

Table 1 – Measurements vs Prediction

The temperature profiles applied to the walls were created by interpolating linearly between the data points from the thermocouples in the test rig. Since no test data for a case without cooling flow was available, from the first phase of the testing, the re-ingestion experiment was added to the data table, as this was considered to be the closest to a fully balanced, un-cooled configuration, as explained by Guijarro et al [17]. The model was then run with these wall temperature profiles for each flow case, and values of fluid temperature were extracted from the CFD solution. A summary of the benchmarking exercise is shown in Table 2. Refer to Figure 19 for the stator well air temperature thermocouple locations (MP No.).

		Test	A	NA	A	NA
	MP No	**T [K]**	**T [K]**	**T [K]**	**ΔT [K]**	
NO COOLING	MP 025	394.6	393.6	393.0	-1.0	-1.6
	MP 026	394.3	394.5	394.8	0.2	0.5
	MP 027	396.5	394.7	396.0	-1.8	-0.5
	MP 028	397.1	394.9	395.8	-2.2	-1.3
	MP 029	397.3	394.7	395.9	-2.6	-1.4
	MP 030	396.4	395.0	396.6	-1.4	0.2
	MP 032	394.4	401.4	393.9	7.0	-0.5
HOLE - 30 g/s	MP 025	393.4	394.1	395.9	0.7	2.5
	MP 026	392.0	393.7	394.8	1.7	2.8
	MP 027	392.0	393.5	394.2	1.5	2.2
	MP 028	391.2	393.1	392.6	1.9	1.4
	MP 029	390.3	392.8	392.1	2.5	1.8
	MP 030	378.3	374.4	380.9	-3.9	2.6
	MP 032	380.6	383.0	382.5	2.4	1.9
SLOT - 30g/s	MP 025	386.3	383.5	387.8	-2.8	1.6
	MP 026	386.2	384.0	387.6	-2.2	1.4
	MP 027	386.2	384.0	387.4	-2.2	1.2
	MP 028	386.0	384.1	387.1	-1.9	1.1
	MP 029	386.0	384.0	387.2	-2.0	1.2
	MP 030	384.7	383.7	386.7	-0.9	2.0
	MP 032	384.8	386.8	386.2	2.1	1.4
HOLE - 55 g/s	MP 025	369.5	351.6	366.3	-17.9	-3.2
	MP 026	367.7	351.5	365.7	-16.2	-2.0
	MP 027	366.5	351.5	363.3	-15.0	-3.2
	MP 028	364.5	351.6	362.0	-12.9	-2.5
	MP 029	364.1	351.8	361.8	-12.3	-2.3
	MP 030	354.3	350.2	356.2	-4.1	1.9
	MP 032	361.1	355.7	364.0	-5.4	2.9
SLOT - 55g/s	MP 025	364.3	346.7	361.1	-17.6	-3.2
	MP 026	366.4	346.5	360.7	-19.9	-5.7
	MP 027	365.3	346.2	360.0	-19.1	-5.3
	MP 028	365.1	346.2	360.4	-18.9	-4.7
	MP 029	365.0	346.2	360.1	-18.8	-4.9
	MP 030	362.7	345.2	360.0	-17.5	-2.7
	MP 032	364.6	348.7	366.8	-15.9	2.2

Table 2: Air temperatures in the cavity

The results have been compared to the adiabatic calculation (A) and the non-adiabatic calculation (NA), in order to assess the importance of the windage heating, relative to the convective heat transfer from the surrounding walls. As seen in Table 2, the application of the measured wall temperature

profiles, i.e. to the 'inside surfaces of the stator well cavity, gives a much closer matching to the test data, showing that the heat pick-up, which raises the air temperature downstream the labyrinth seal, is counteracted by the heat loss from the fluid to the cavity walls. The temperature of the cavity walls must be fairly well defined, in order to predict the right level of air temperature within the stator well cavity.

When the heat transfer is neglected across the cavity walls, the expected temperature drop does not occur in the stator well cavity air flows, and the inner wall temperatures are overestimated. At this stage in the project, heat flux profiles were being extracted from the CFD solution and fed to the FE code 'manually', in order to produce a coupled result (one iteration). Overall the 'manually coupled' CFD/FE method predicts the stator well air temperatures to an acceptable accuracy, if the prescribed wall temperatures are about right.

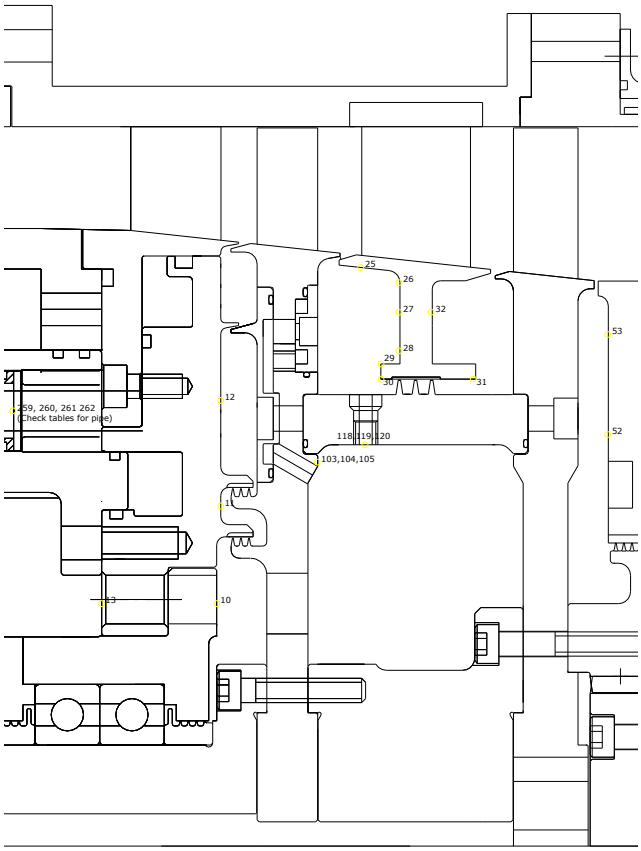

Figure 19 Air temperature measurement locations

Metal temperature validation based on manual matching.

For the next step in the preparation of an improved coupling model, a similar approach was adopted but now the measured temperature profiles were applied to the more remote boundaries of the FE SC03 model. In these calculations the boundary conditions around the outer extent of the FE model, rotor 1 disc front face, rotor 2 disc rear face, etc. were applied using conventional heat transfer correlations, and an initial matching of the thermocouples around the stator well cavity was conducted. This was done for the case of no cooling flow in the 2D FE model. A 'perfect' matching was not possible for all thermocouples, as it was anticipated that the use of an automated coupling approach would be required to produce the best solution. This was reported in [5].

Automated coupling 3D CFD and 2D SC03 with no cooling flow.

The remaining problems with the automated coupling method were later resolved as reported by Guijarro in [6]. Figure 20 shows results for the automated coupling approach, i.e. 3D CFD to 2D axisymmetric FE un-cooled case.

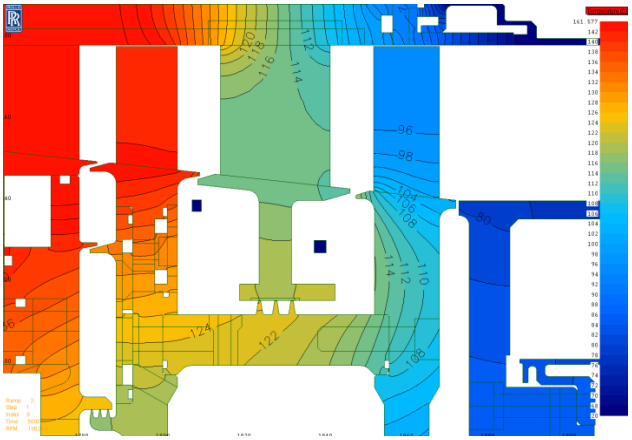

Figure 20 – Contours of metal temperature for the coupled solution using the 2D SC03 model and a reduced 3D CFD model - uncooled.

The coupled predictions are very accurate in most places, the differences being below 2K, and capture the gradients in areas of high recirculation. The biggest discrepancies were found near the rim gaps, where the mixing of the air with the main stream was not reproduced as accurately. It is also important to note that the main annulus boundary conditions were extracted from the CFD analysis, but still relying on modified empirical correlations to reapply them to the FE model. The 3D to 3D coupling overcomes this requirement as explained later in this paper.

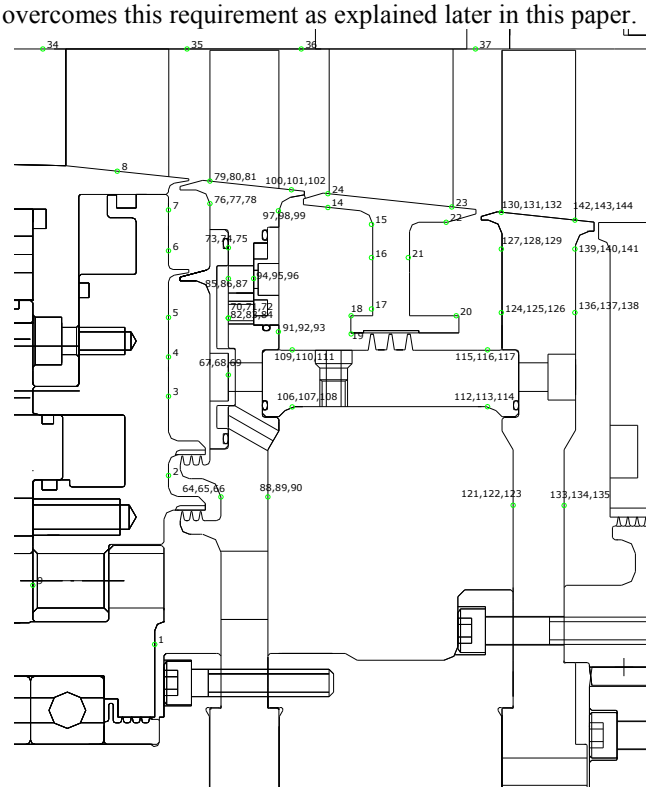

Figure 21 Metal temperature measurement locations

The results of the 3D CFD to 2D FE automated coupling, comparing predicted and measured metal temperatures at positions shown in Figure 21, are given in

Figures 22, 23 and 24, i.e. comparing HYDRA and Fluent based automated coupled solutions, with test data. Also shown are the earlier, manually coupled predictions.

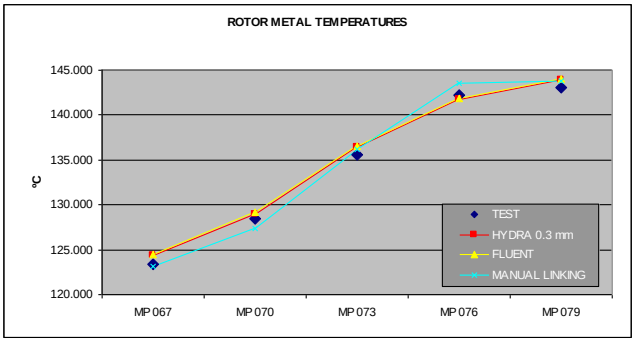

Figure 22 – Metal temperature chart of the Stage 1 rotor disc front thermocouples

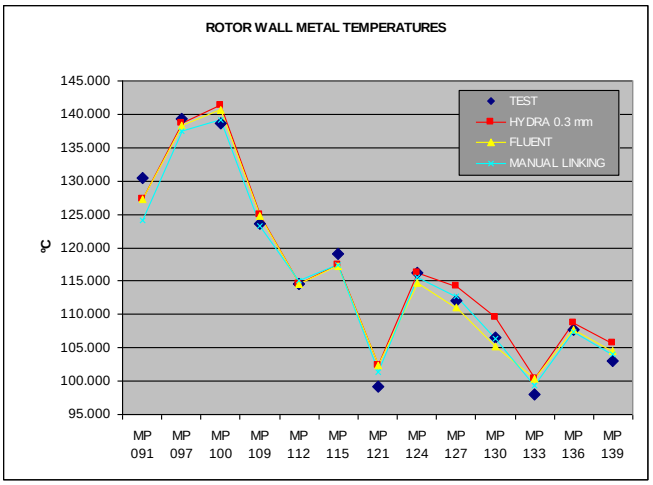

Figure 23 – Metal temperature chart of the Stage 1 rotor disc rear thermocouples

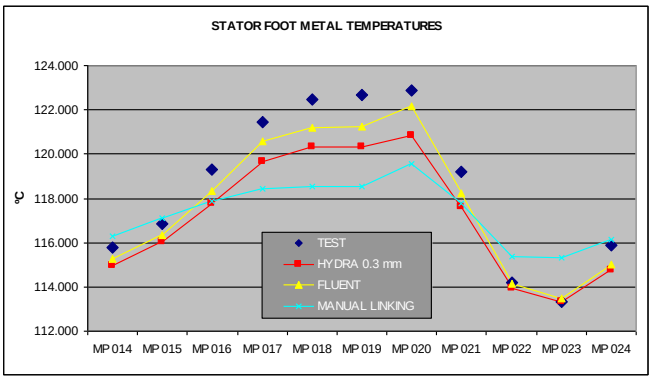

Figure 24 – Metal temperature chart in the inter-stage seal stator foot wall thermocouples

Figure 25 shows combined contours of non-dimensional metal temperature in the metal, (right hand side key), and the air (bottom key), for the coupled solution. The combined illustration allows us to make a simultaneous description of the interaction between the fluid and solid, as produced by the coupling process. The air ingested in the cavity is cooler with respect to the rotor disc, as it has lost energy in the turbine blade. When entering the cavity, the fluid attaches to the stator foot wall, and will heat up the static part of the cavity. Then this air re-circulates in the cavity, heated up by the viscous work done by the rotor, as well as the advection from the rotor disc. The mass flow through this recirculation has been calculated at almost twice the flow predicted by the free disc entrainment correlation, i.e. 84.15 g/s of main stream flow in the re-circulation, compared to 43.6 g/s free disc entrainment at this location.

The calculations showed that for this uncooled cavity case, 40.1 g/s of the main stream flow will be demanded by the labyrinth seal. This air is then further heated up in the labyrinth seal, before being vented back to the main annulus, in front of the stage 2 disc rim. Note that this hot air created a radial gradient of temperature in the stator foot, being hotter at the inner diameter than at the blade platform.

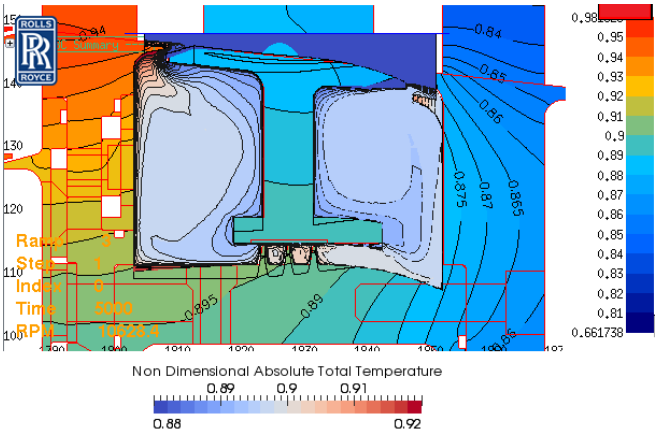

Figure 25 - Non dimensional temperature contours in the metal and air showing the heat transfer mechanism predicted by the coupled analysis.

3D/3D Automated Coupling Un-cooled

The next step was to produce a coupled model, including the main annulus (stator), which has the advantage of moving the boundary conditions further away from the thermocouple measurements i.e. more of the FE model boundary conditions are generated directly by the CFD solution. Figure 26 shows 3D metal temperature contours comparing the test data measurements and the predicted values of metal temperature. The results are comparable to the 3D to 2D coupling.

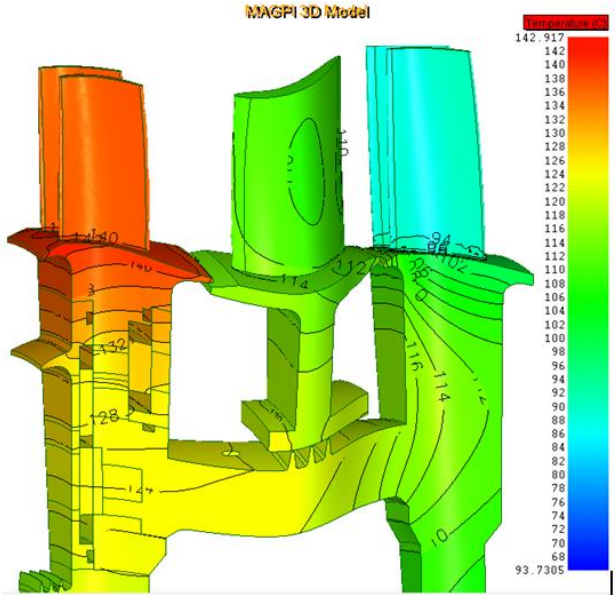

Figure 26 – Contours of metal temperature for the coupled solution using the 3D SC03 model and the cut down 3D CFD model for an un-cooled configuration.

As expected the prediction accuracy for the 3D/3D solution is improved as summarized in Figures 27 to 29.

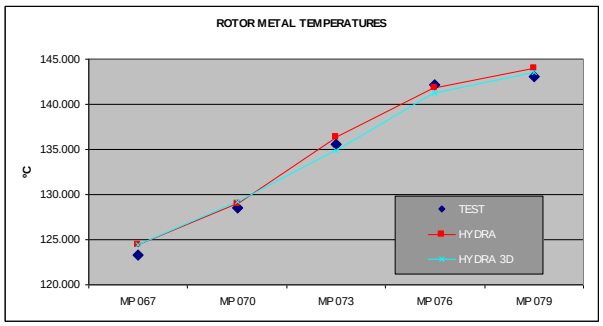

Figure 27 – Metal temperature chart in the Stage 1 front face disc thermocouples comparing the 2D and 3D cases with the test data.

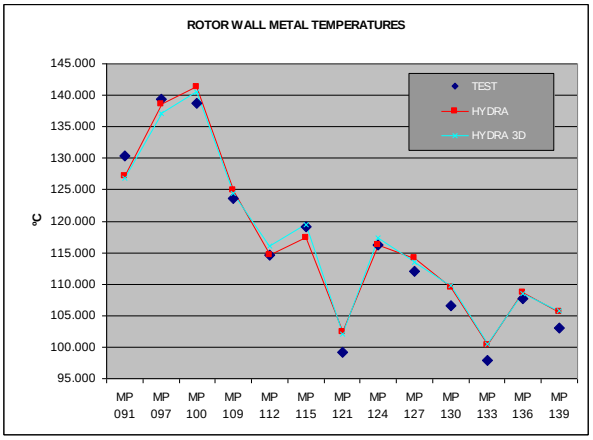

Figure 28 – Metal temperature chart of the Stage 1 rotor disc rear thermocouples comparing the 2D and 3D cases with the test data.

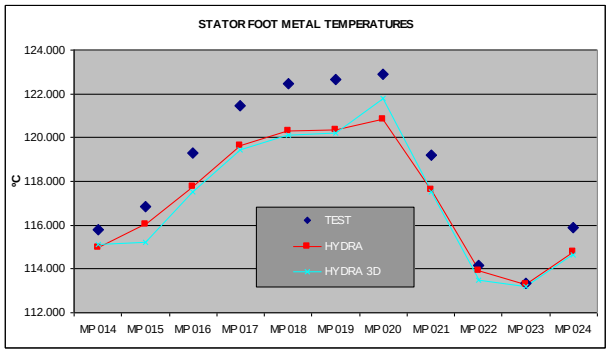

Figure 29 – Metal temperature chart in the stator foot thermocouples comparing the 2D.and 3D cases with the test data.

The effect of interstage seal clearance

The rig was equipped with a displacement sensor which showed an important variation of the seal clearance under certain operating conditions. This indicated that an additional coupled analysis for the un-cooled case was required, with an increased hot running seal clearance.

The CFD results give an indication of the effects of seal running clearance on metal temperatures in the stator well cavity. The ingested air is heated up in the upstream cavity before flowing through the labyrinth seal. The air flows through the seal due to the pressure drop across the NGV. This air then flows into the downstream cavity. The fluid temperature rise due to windage heating, through the seal is less, due to increased mass flow. Thus the temperature at the front face of rotor 2 is lower than in the case with a smaller seal clearance. If the clearance is set too high in the coupled analysis, the predicted fluid temperatures, relative to measured data, would be too low. The adiabatic CFD results performed to-date, show that the levels of ingestion are higher with increased seal clearance, and the changes in flow patterns, (see Figures 30 and Figure 31), modify the heat transfer distribution in the cavity.

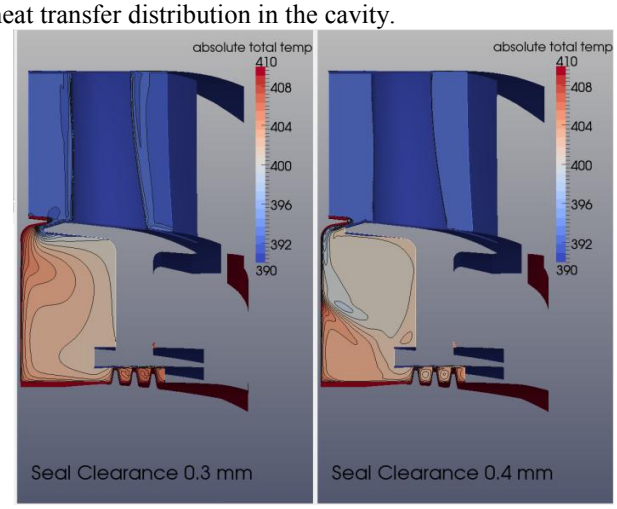

Figure 30 – Absolute total temperature contours in the stator well cavity (un-cooled)

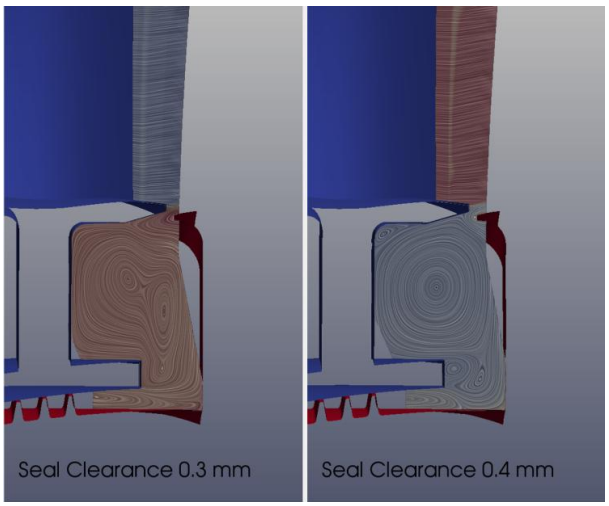

Figure 31 – Path lines un-cooled cavity

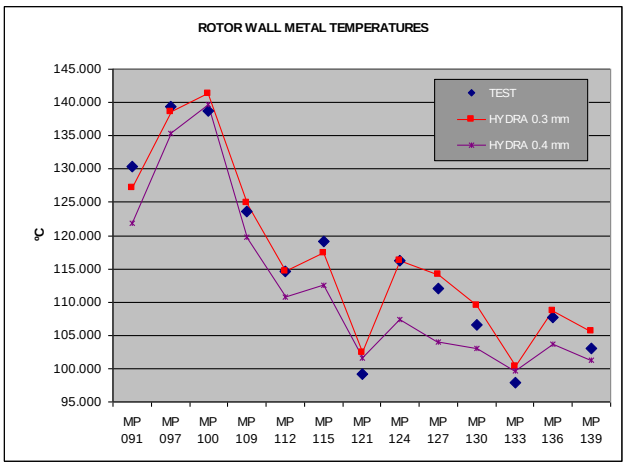

Figure 32 – Metal temperature chart in the Stage 1 rotor disc rear thermocouples comparing the effect of the seal clearance with the test data. Un-cooled cavity.

Figure 32 shows the effect of the seal clearance on disc rotor temperatures. This result is particularly important, as it shows that the coupling can be used to assess the accuracy of the seal clearance predictions.

Cooled case coupled model

The final step was to extend the coupled model to cover the cooled cavity condition, including the blade passages and extending the boundary conditions to the inlet of the main gas path test section. This example provides even better validation, as the thermal gradients in the cavity are higher, and the case is more representative of the more significant engine conditions.

Figure 33 shows contours of metal temperatures in the assembly, for the 55 g/s cooling air supply case. This shows that the coolant has flooded the cavity, and the temperatures are lower than previous cases.

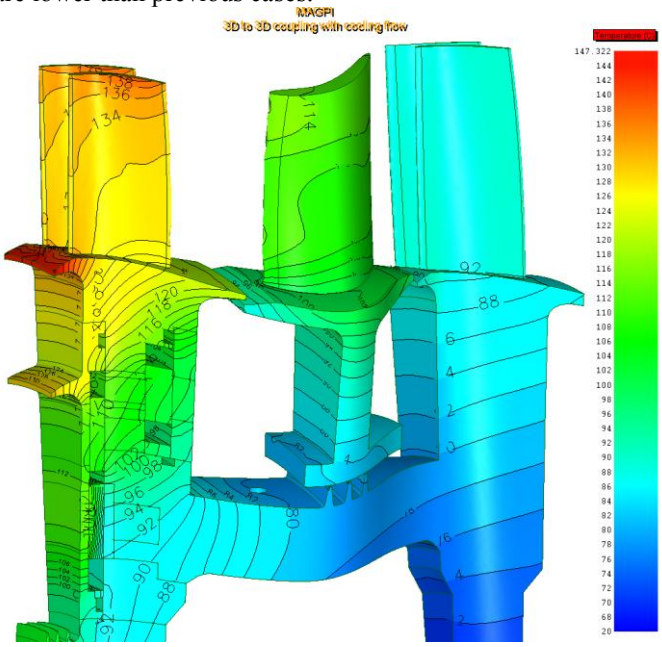

Figure 33 – Contours of metal temperature for the coupled solution using the 3D SC03 model and the whole 3D CFD model, for the cooled case.

The comparisons to test data, shown in Figure 34, are also encouraging, although some discrepancies can still be found, especially near the rim gap regions. Again, the differences are within 2K, except in the vicinity of the rim gaps, showing the potential of the CFD/FE coupling methodology.

However, in the problem areas (rim gaps), the following actions could improve the coupling still further by adjusting the seal clearance in line with more recent measurements [18] and exploring the use of enhanced turbulence models. These should improve the modelling of the mixing, and the ingestion, near the rim gaps. LES (Large Eddy Simulation) is also thought likely to improve the modelling accuracy; O'Mahoney [19]. In addition the use of 'hot running' geometry in the coupled solution and possibly working with unsteady solutions, including coupling, are likely to provide some improvement.

Cooling 'Optimisation'

Having established the credibility of CFD solutions for heat transfer in this type of cavity, an investigation into the effects of cooling air mass flow level, has been carried out, with the multiple reference frame CFD models, (steady, adiabatic solution); recognizing that there will be some quantitative limitations on the predictions of gas ingestion, but anticipating that qualitative results will give a good indication of the better cooling arrangements.

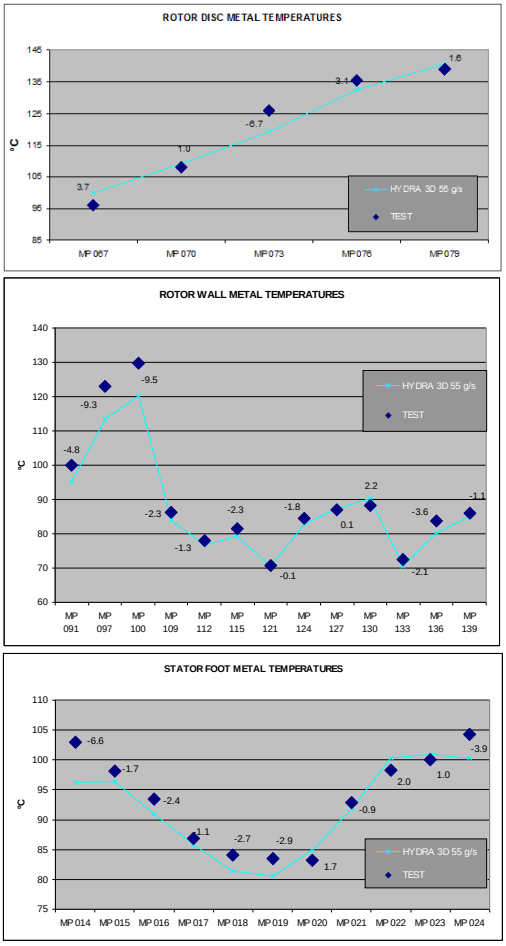

Figure 34 3D model Cooled case comparisons

Optimised Cooling Studies

To help with this objective, a 'measure' of this cooling performance has been established, as described in equation (1), i.e. thermal cooling effectiveness; see [5 and 6].

$$\eta_{eff} = \frac{T_{hot} - T_{wall}}{T_{hot} - T_{cool}} \quad (1)$$

Where *hot* denotes the inlet total temperature to the rig in Kelvin, and *cool* the relative total temperature of the cooling flow, at the chosen delivery option inlet. In addition, a calculation of turbine stage efficiency was performed, which was expected to follow a trend in the reduction of stage efficiency, with additional cooling air efflux. The isentropic efficiency of the turbine rig is calculated automatically by HYDRA using the expression described in equation (2).

$$\eta = \frac{\left\{ \sum_{i=inlets} (\dot{m}H_0)_i - \sum_{i=exits} (\dot{m}H_0)_i \right\}}{\left\{ \sum_{i=inlets} (\dot{m}H_0)_i - \sum_{i=secondary\ exits} (\dot{m}H_0)_i - (\dot{m}H_{0_{ideal}})_{main\ exit} \right\}} \quad (2)$$

Here the ideal exit total enthalpy is calculated by isentropically expanding each gas stream to the total pressure of the mainstream rotor exit. The flow aerodynamics inside the cavity have been studied by looking at the path-lines and contours of cooling effectiveness, at the rear face of the rotor 1 disc wall. As an example, Figure 35 shows this parameter, for each geometry configuration at the 30 g/s cooling flow case. It is evident from this study that, the cooling effectiveness can be significantly improved with relatively minor changes to the local geometry.

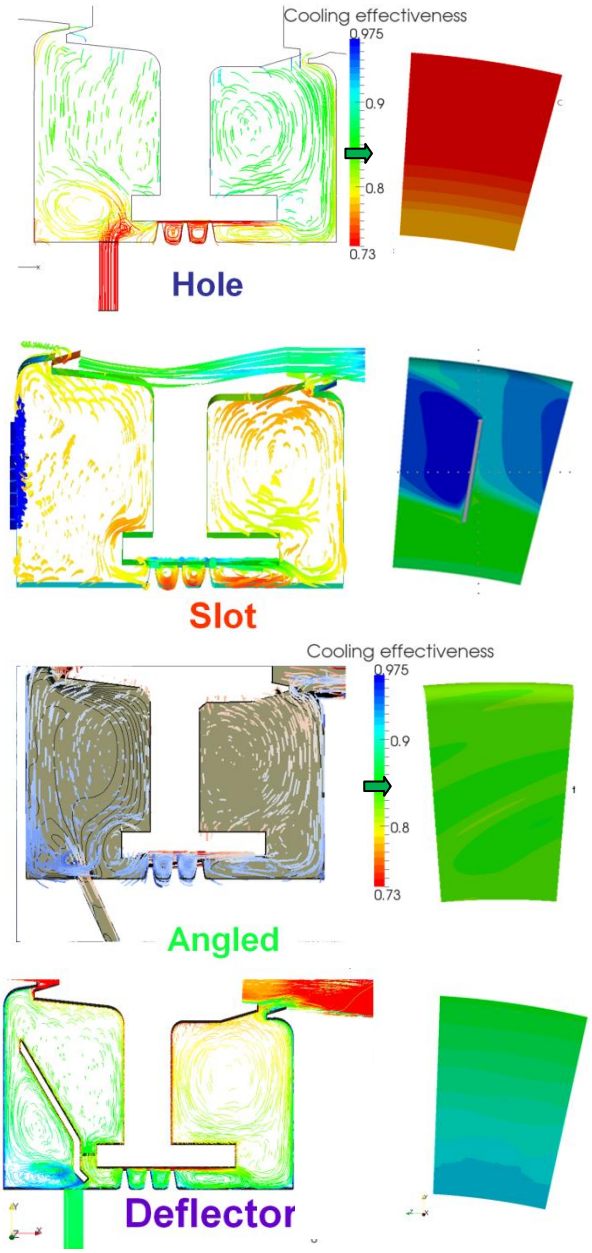

Figure 35 cooling effectiveness at 30 g/s

For this flow case, the labyrinth seal demand is higher than the coolant supply, resulting in hot gas ingestion, which after coming radially into the cavity and mixing with the cooling air, flows directly towards the downstream cavity through the interstage seal. This risks a significant reduction in cooling effectiveness. When the flow is injected axially through the lock-plate slot, the coolant creates a "protective" film, which is entrained into the disc pumping flow. The ingestion is reduced and the cooling effectiveness is improved, at the important rear face of the rotor disc.

For the second phase of rig experiments, a different cavity configuration, using an angled insert which deflects the air towards the rotor, was tested. The effect of this expected change is predicted here, (adiabatic solution only at this stage). The jet from the angled holes reaches the rear face of the rotor and cools the disc rear face, moving helicoidally inside the cavity. The coolant is used more effectively, and achieves improved sealing of the up-stream cavity. However, there is still some ingestion which affects the stator foot, and which mixes with the coolant in the cavity, achieving lower values of cooling effectiveness.

Also included in the second round of experiments, was the static deflector plate. The CFD analysis shows the coolant confined near the disc rear face, which is then pumped radially outboard, i.e. to the rim gap region. The benefits of this configuration are obvious as, for this low cooling flow case; the device manages to prevent the ingested hot gas mixing with the cooling flow, where it matters, by directing the hot gas away from the rotating components. In the experimental work, a wider range of flow cases was run, also covering cases with no ingestion. This has also been covered in the CFD analysis. To allow easy benchmarking between the different configurations, the value of cooling effectiveness was integrated across the rear face of the disc, in order to achieve a 'figure of merit' for this comparison. The values are plotted in Figure 36.

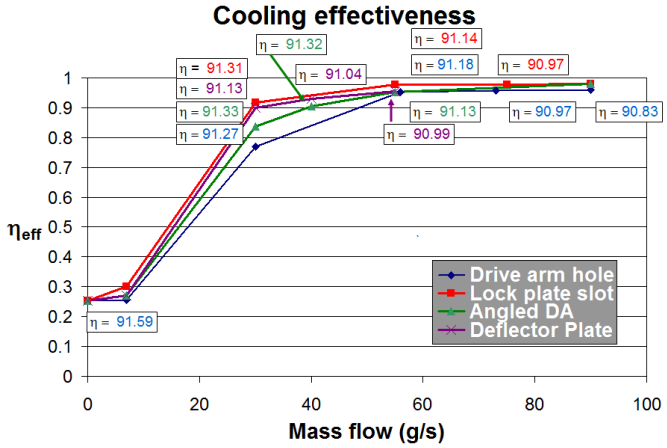

Figure 36 - Cooling effectiveness - rotor 1 rear face

The chart shows that for values of cooling flow over 55 g/s, (more than the inter-stage seal demand), the excess of air does not produce any benefit in terms of cooling effectiveness, and there is a penalty in turbine efficiency due to 'spoiling' of the main annulus flow. For the lower, (more typical), cooling air supply case (30 g/s), the worst configuration is the radial drive arm hole, which achieves less than an 80% level cooling effectiveness, and still allows some local ingestion of hot gas into the cavity. Indeed, a mass flow rate over 50 g/s is required to achieve adequate sealing of the cavity. When angling the hole, a better cooling effectiveness is achieved. The deflector plate and the lock plate slot produce similar levels of cooling effectiveness, the lock-plate slot being the most effective configuration, by a small margin, probably within the CFD modelling accuracy.

The lock-plate slot result shows no significant reduction in turbine efficiency, for the improvement it provides in cooling effectiveness. However the deflector plate configuration, incurs a small penalty in turbine stage efficiency, as it pumps the air with a strong radial component of jet momentum, back into the main annulus flow. Additional design considerations must be taken into account, in order to decide the best possible configuration. Whilst the simpler drive arm hole configuration is not ideal for cooling effectiveness, the choice between the deflector plate and the lock-plate slot configurations requires further analysis in other fields. The main objectives here have been to reduce disc rim temperatures for a given cooling flow, also improving the SFC, hence cost, stress, weight and life analyses are also required in the real gas turbine world.

CONCLUSIONS

The MAGPI research programme is now complete and the results obtained from the work-package covering turbine stator well heat transfer have produced some encouraging results. A coupled CFD/FE modelling capability has been established for convective heat transfer in the complex flow fields of turbine stator wells, and this methodology has been adequately validated for a representative geometry and a range of flow cases.

The coupled CFD/FE analysis has allowed us to use disc surface temperature measurements to adequately validate the predicted convective heat transfer in the stator well cavity, including the complex flow situations present in cooled stator well cavities with local gas ingestion at the disc rim gaps, i.e. up to the radial locations typical of disc rims and blade fixings, even if the precise levels of annulus gas ingestion, in the region of the rim gaps, is less well captured by the relatively simple RANS CFD modelling method.

This has allowed us to have reasonable confidence in using the less expensive and less time consuming adiabatic CFD solutions, to investigate with confidence a range of design alternatives in order to select the most promising cooling configurations. In this case the 'lock-plate slots' and the static deflector-plate were shown to be the better options in terms of cooling effectiveness. In the more detailed design phase of a 'real' project the coupled CFD/FE solution would be deployed in order to obtain the best possible understanding of the disc rim and blade fixing temperature predictions, in support of stress and life analyses.

Further exploitation activity is now anticipated from the partners involved in the programme, which is already resulting in significant patent applications in preparation for applying the technologies demonstrated, into future engine projects. This is expected to deliver the benefits of reduced fuel consumption and emissions that go with the improvements to the engine performance resulting from reduced cooling air consumption.

ACKNOWLEDGMENTS

The present investigations were supported by the European Commission within the Framework 6 Programme, Research Project 'Main Annulus Gas Path Interactions (MAGPI)', AST5-CT-2006-030874. This financial support is gratefully acknowledged. Thanks also to our university and industrial partners at The University of Florence, The University of Sussex, The University of Surrey, Avio (Italy), MTU (Germany), Siemens (UK) and Turbomeca (France).

A special mention must also be made to Rolls-Royce colleagues Christopher Barnes and Leigh Lapworth for their technical support, advice and recent developments of the analysis codes and plugins (Hydra and SC03).

REFERENCES

[1] SPECIFIC TARGETED RESEARCH PROJECT *Annex I – "Description of Work"*. Project acronym: MAGPI. Project full title: Main Annulus Gas Path Interactions. Proposal/Contract no.: 30874 Date of preparation of Annex I: May 2006

[2] Jeffrey A. Dixon, Ivan L. Brunton, Timothy J. Scanlon, Grzegorz Wojciechowski Vassilis Stefanis, Peter R. N. Childs "Turbine stator well heat transfer and cooling flow optimisation" ASME paper GT2006-90306.

[3] J.Illingworth, N.Hills, C.Barnes, "3D Fluid-Solid Heat Transfer Coupling of an Aero-engine Preswirl System", ASME Gas Turbine Conference 2005

[4] Peter E. J. Smith, Jon Mugglestone, Kok Mun Tham, Daniel Coren, Daniel Eastwood and Christopher Long. "Conjugate Heat Transfer CFD Analysis in Turbine Disc Cavities" ASME Paper GT2012-69597.

[5] Jeffrey A. Dixon, Antonio Guijarro Valencia, Andreas Bauknecht, Daniel Coren, Nick Atkins "Heat Transfer in Turbine Hub Cavities Adjacent to the Main Gas Path" ASME Paper GT2010-22130.

[6] A Guijarro Valencia, Jeffrey A. Dixon, Attilio Guardini, Daniel Coren, Nick Atkins "Heat Transfer in Turbine Hub Cavities Adjacent to the Main Gas Path Including FE-CFD Coupled Thermal Analysis" ASME Paper GT2011-45695

[7] Coren, D. D., Atkins, N. R., Childs, P. R. N., Turner, J. R., Eastwood, D., Davies, S., Dixon, J., Scanlon, T. "An Advanced Multi Configuration Turbine Stator Well Cooling Test Facility", Paper Number GT2010-23450ASME, in proceedings of the ASME Turbo Expo 2010, Glasgow, UK, June 14-18 2010.

[8] Eastwood D., Coren D. D., Long C. A, Atkins N.R., Turner J. R., Childs P. R. N., Scanlon T. J., Dixon J. A., Guijarro Valencia, A. "Experimental Investigation Of Turbine Stator Well Rim Seal, Re-ingestion and Interstage Seal Flows Using Gas Concentration Techniques and Displacement Measurements" ASME Paper GT2011-45874.

[9] Z.Sun, J.Chew, N.Hills, K.Volkov, C.Barnes, "Efficient FEA/CFD thermal coupling for engineering applications", ASME Gas Turbine Conference 2008. ASME Journal of Turbomachinery.

[10] D.Amirante, N.Hills, "A Coupled Approach for Aerothermal Mechanical Modelling for Turbomachinery", 1st International Conference on Computational Methods for Thermal Problems, 2009

[11] Verdicchio, J. A., "The validation and coupling of computational fluid dynamics and finite element codes for solving industrial problems". DPhil Thesis, University of Sussex, July 2001.

[12] Edmunds T., "Practical three dimensional adaptive analysis". In Proceedings of 4th International Conference on Quality Assurance and Standards, NAFEMS, 1993.

[13] FLUENT Inc. Lebanon, New Hampshire.

[14] Lapworth, L. The Hydra's User Guide for version 6.1.7 beta. Rolls-Royce plc, 2009.

[15] Da Soghe, Andreini, Facchini "Turbine stator well CFD studies: Effects of coolant supply geometry on cavity sealing performance", ASME TurboExpo 2009 GT-2009-59186

[16] Spalart, P. R., and Allmaras, S. R., "A One-Equation Turbulence Model for Aerodynamic Flows," AIAA 92-0439, 1991

[17] Guijarro et al "An Investigation into Numerical Analysis Alternatives for Predicting Re-ingestion in Turbine Disc Rim Cavities", ASME TurboExpo 2012paper GT-2012-68592

[18] Eastwood, D; Coren D D; Childs, P; Guijarro Valencia, A; Scanlon, T; Dixon, J A, "Experimental Investigation of Turbine Stator Well Rim Seal, Re-Ingestion and Interstage Seal Flows Using Gas Concentration Techniques and Displacement Measurements" ASME Journal of Turbomachinery GTP-11-1221

[19] O'Mahoney, T S D; Hills, N J; Chew, J W and Scanlon, T. "Large-Eddy simulation of rim seal ingestion" Proceedings of the Institution of Mechanical Engineers.

